IJCA

Indonesian Journal of Chemical Analysis

Homepage: https://journal.uii.ac.id/IJCA

Direct Cu, Fe, and Ni Ions Multicomponent Analysis Using UV-Vis Spectrophotometric Method

Suprapto Suprapto[a,*], Yatim L. Ni'mah[a], Feraldy A. Putrama [a]

[a] Chemistry Department, Institut Teknologi Sepuluh Nopember, Surabaya, Indonesia
*corresponding author: suprapto@chem.its.ac.id
DOI: 10.20885/ijca.vol6.iss2.art2

ARTICLE INFO

Received : 01 May 2023
Revised : 22 May 2023
Published : 01 September 2023
Keywords : UV-Vis Spectrometry, Multicomponent Analysis, Cu(II), Fe(III), Ni(II).

ABSTRACT

This study presents a direct multicomponent analysis method using UV-Vis spectrophotometry to determine Cu(II), Fe(III), and Ni(II) ion content without prior complexation or separation. Single and multivariate regression was used to predict metal ion content, and the resulting model was trained and validated using a dataset of 25 multi-component samples. The mean recoveries for Cu(II), Fe(III), and Ni(II) using linear and ridge regression based only on absorbance at 805 nm were 99.97% and 101.6%, 95.42% and 95.65%, and 99.43% and 99.99%, respectively, for the 20% test data. The mean recoveries for Cu(II), Fe(III), and Ni(II) using linear and ridge regression based only on absorbance at 805 nm were 92.27% and 95.03%, 125.3% and 124.11%, and 104.15% and 105.52%, respectively, for the test solution outside of the training data. These results demonstrate the effectiveness of the multivariate UV-Vis spectrophotometric method for the simultaneous determination of Cu(II) and Ni(II) in multicomponent samples, which meets the analysis standard and can be successfully applied. Finally, the study sheds light on the influence of spectral interference on the accuracy of regression models. It highlights the importance of carefully selecting the wavelengths used as predictors in such models. This can have significant implications for developing and validating analytical methods, particularly in cases where multiple analytes were present in a sample.

1. INTRODUCTION

The analysis of metal ions in multicomponent samples offers significant advantages in terms of measurement efficiency. Numerous studies have been conducted to investigate the content of mixed metal ions in different contexts. For instance, Chen et al. (2019) optimized the decomposition and purification process of zinc metal by analyzing the content of Co(II) and Cu(II) in a concentrated zinc sulfate solution [1]. Similarly, Xu et al (2014). performed a quantitative analysis of Cd(II), Zn(II), and Co(II) in drinking water to mitigate their adverse effects and control the levels of metal ions that are considered safe for consumption. The need for simultaneous analysis of mixed metal ion samples in various fields has led to the continuous development and refinement of analytical methods to ensure their accuracy and reliability [2-4].

Various spectrophotometric methods, such as atomic absorption spectroscopy (AAS) [5], atomic fluorescence spectroscopy (AFS) [6], and UV-Vis spectrophotometry [7], as well as other analytical techniques, have been used to quantitatively analyze mixed metal ion samples. Among these methods, UV-Vis spectrophotometry is one of the most extensively employed techniques, and

its application has been developed for the simultaneous quantitative analysis of metal compounds and other compounds. This method is favored by many researchers because it is easy to use, fast, accurate, and efficient [1].

To improve the accuracy and stability of UV-Vis spectral analysis, various pretreatment methods have been developed to overcome overlapping spectra of multiple metal ions and minimize noise. Chemometric methods such as PCR, PLS regression, and multivariate regression have been applied to the simultaneous quantitative analysis of mixed metal ion samples. Variable selection methods have improved measurement accuracy and stability. This study focused on developing a reliable and accurate method for the determination of Cu(II), Fe(III), and Ni(II) using UV-Vis spectrophotometry [8-10].

This study presents an innovative and effective method for simultaneously determining Cu(II), Fe(III), and Ni(II) ions in aqueous solutions utilizing UV-Vis spectroscopy and regression models. The proposed method offers numerous benefits, including its simplicity, cost-effectiveness, and minimal sample preparation requirements, rendering it well-suited for routine analysis across diverse fields such as environmental monitoring, industrial process control, and quality assurance in the pharmaceutical and food industries. Notably, this method stands out from traditional metal analysis approaches employing UV-Vis spectrophotometers that often involve complexation processes to achieve accurate results [11-13]. A key focus of this study was to compare the performance of linear regression and ridge regression models in predicting the concentrations of the target metal ions based on their absorbance values at specific wavelengths. Furthermore, the impact of one ion's absorption on the prediction of another ion was examined using only three estimators. Ridge regression was found to be a valuable tool for enhancing the accuracy and precision of regression models, particularly when addressing multicollinearity issues present in spectral data. Overall, this study offers valuable insights into the development of a robust method for simultaneous ion determination, highlighting the significance of ridge regression in refining regression models and underscoring the negligible impact of one ion's absorption on the prediction of another.

2. EXPERIMENTAL METHOD

2.1. Materials and Instruments

In this study, various apparatus and materials were used. The apparatus used included glassware, an analytical balance, a micropipette, a 10 mm quartz cuvette, and a UV-Visible spectrophotometer (Genesys 10S). Meanwhile, the materials used were $CuSO_4.5H_2O$ (SAP Chemicals, >99%), $FeCl_3.6H_2O$ (SAP Chemicals, >99%), $NiCl_2.6H_2O$ (SAP Chemicals, >97%), and demineralized water (Brataco chemical). All the chemicals were purchased from a local store in Surabaya, Indonesia, and were used without any further purification.

2.2. Methods

In this study, the standard solutions were prepared by mixing different volumes of metal ion stock solutions and then diluting the mixed solution with demineralized water to obtain a multi-component solution with final concentrations of Cu(II), Fe(III), and Ni(II). The concentration ranges of the metal ions in the multi-component solution were Cu(II) 3-5 g/L, Fe(III) 0.010-0.002 g/L, and Ni(II) 7-11 g/L, as shown in Table 1. The absorption spectra of the multi-component solution were measured using a UV-Vis spectrophotometer in the wavelength range of 200-1000 nm with demineralized water as a blank. Triplicate measurements were carried out to obtain accurate and reliable data.

2.3. Multivariate Regression

Multivariate regression analysis was used to analyze the multi-component training datasets, and the obtained regression model was utilized to predict the concentrations of Cu(II), Fe(III), and Ni(II) in the test solution. The multivariate regression equation was simplified as Eq. (1), where the dependent variable was yn, the independent variables were xn, B represented the intercept, and An was the regression coefficient. The error C was assumed to be 0 or E(C) = 0 in classical regression, but multivariate regression considered more perspectives to solve correlation problems, such as collinearity, inflation of variance, and insignificant dependent variables, among others [14].

$$y\_n = A\_1\ x\_1 + \cdots + A\_n\ x\_n + B + C \quad (1)$$

2.4. Ridge Regression

Ridge regression is a regularization technique used in linear regression models to address the problem of multicollinearity, which occurs when there is a high correlation among predictor variables. It is particularly useful when dealing with datasets where the number of predictors is larger than the number of observations or when predictors are highly correlated.

The basic idea behind Ridge regression is to introduce a penalty term to the ordinary least squares (OLS) cost function. This penalty term is determined by the hyperparameter α (alpha) and is added to the sum of squared residuals in the cost function. The cost function of Ridge regression can be represented as in equation (2):

$$\text{Cost} = \text{RSS} + \alpha * \Sigma(\beta\text{^}2) \quad (2)$$

Here, RSS is the residual sum of squares, β represents the regression coefficients, and Σ(β^2) is the sum of squared coefficients. The term α controls the amount of regularization applied to the model. A larger α value increases the penalty and results in smaller coefficient estimates, which helps reduce the impact of multicollinearity. To estimate the regression coefficients in Ridge regression, a technique called the method of shrinkage is used. It involves minimizing the cost function by adjusting the values of the regression coefficients. The solution is obtained through optimization algorithms such as gradient descent or matrix inversion [15].

3. RESULTS AND DISCUSSION

The absorption spectra of metal ions can vary depending on their chemical form and surrounding environment. Therefore, it is necessary to carefully select the appropriate wavelengths for analysis and consider any potential interferences or overlapping spectra from other ions in the sample. In this study, the absorption spectra of the individual metal ions were used to develop a multivariate regression model for the simultaneous quantification of Cu(II), Fe(III), and Ni(II) in mixed solutions. The individual metal ion spectra of Cu(II), Fe(III), and Ni(II) in mixed solutions were shown in Figure 1.

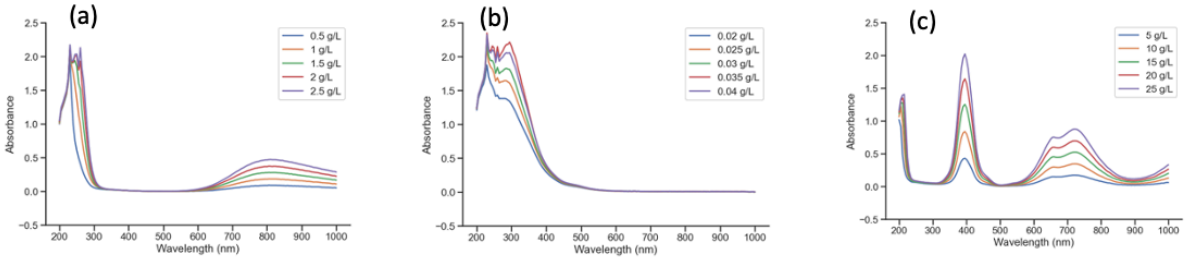

Figure 1. The absorption spectra of (a) Cu(II), (b) Fe(III), and (c) Ni(III).

Figure 1 indicated that Cu(II) and Fe(III) have absorbance peaks at 805 and 295 nm, respectively. While, Ni(II) has three prominent peaks at 495, 660, and 720 nm. The nitroso complex of zinc, nickel, and copper have the maximum peaks at 442, 455, and 492 nm, respectively [2]. The regression curves of individual Cu(II), Fe(III), and Ni(II) at 805 nm, 295 nm, and 395 nm as a function of concentration, were shown in Figure 2. The concentration required to obtain a linear curve for Cu(II), Fe(III), and Ni(II) salts was higher than their complex form [2-5]. But, in terms of sample preparation direct Cu(II), Fe(III), and Ni(II) salts were simpler and did not require a buffer solution. Thus, this method was very promising for routine analysis in metal pickling wastewater or electroplating metal concentration monitoring.

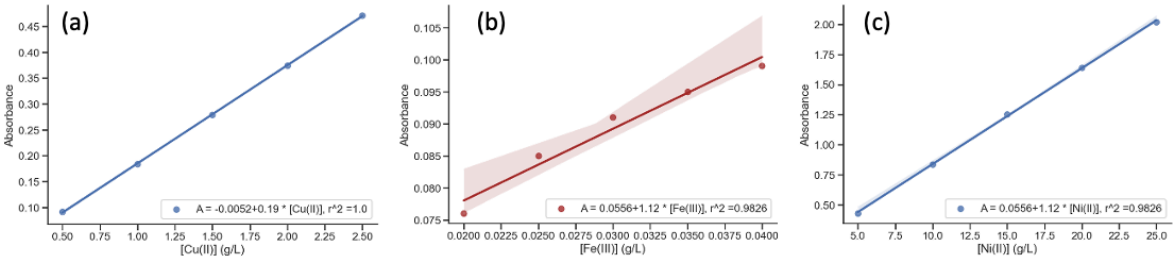

Figure 2. The regression curve of (a) Cu(II), (b) Fe(III), and (c) Ni(III)

The absorption spectra of 25 multicomponent training set solutions were shown in Figure 3(a). Figure 3(b) was the overlay of individual spectra of Cu(II), Fe(III), and Ni(II). It can be seen that the spectra of each metal ion overlap each other. This means that the absorption of each metal ion has been influenced by the other metal ion, so, it was considered that determining the concentration of one metal ion should involve the additive absorbance from the others.

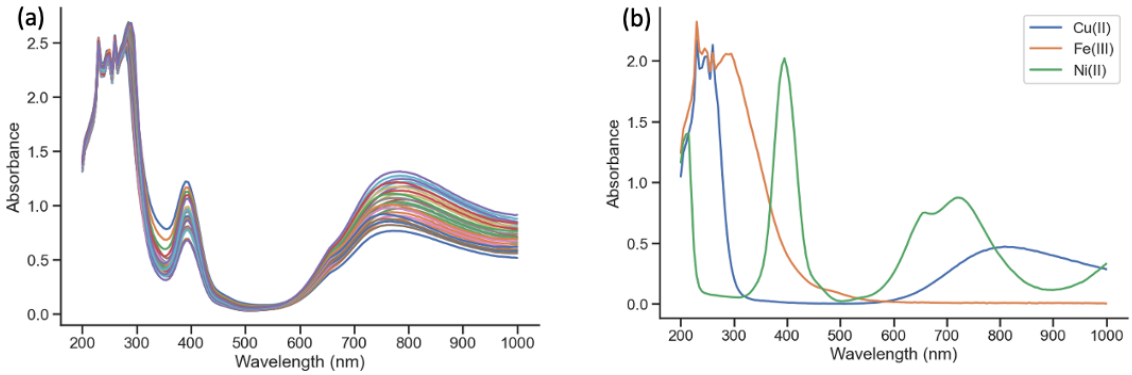

Figure 3. Absorption spectra of 25 multicomponent solutions (a) spectra overlay of Cu(II), Fe(III), and Ni(II) (b)

The absorbances at 805, 720, and 295 nm showed correlation coefficients of 0.96, 0.85, and 0.53, respectively, with variations in Cu(II) concentrations. In contrast, absorbances at these same wavelengths showed correlation coefficients of -0.96, -0.85, and -0.53, respectively, with variations in Fe(III) concentrations, indicating an inverse correlation between the two metal ions. Ni(II) concentrations were well-correlated with absorbances at wavelengths 295, 495, 395, and 720 nm, with correlation coefficients of 0.83, 0.76, 0.98, and 0.53, respectively, as shown in Figure 4.

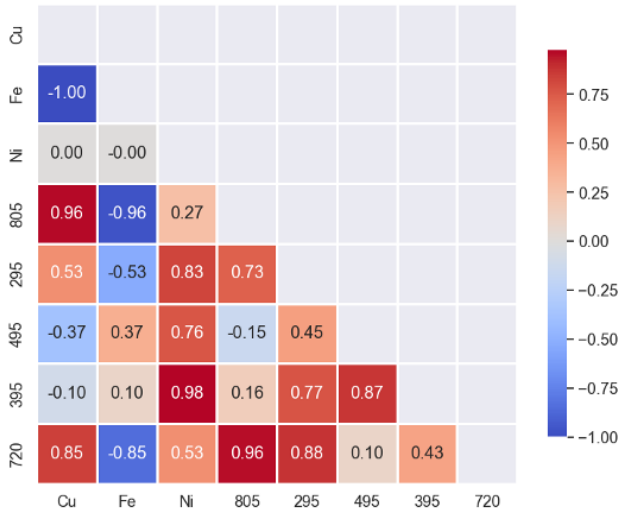

Figure 4. The correlation coefficient between the concentration of Cu(II), Fe(III), and Ni(II) and the absorbance at 805, 295, 495, 395, and 720 nm

The correlation between absorption and concentration at 495 nm was less significant for Cu(II) and Fe(III), although Ni(II) showed a correlation of 0.76. Ni(II) had a stronger correlation with absorption at 295 and 395 nm, which were present in Ni(II) individual spectra. The absorbance at 720 nm, which served as a marker for Ni(II), had a correlation of 0.85 with Cu(II), even though it did not appear in the individual Cu(II) spectra. Fe(III) showed a negative correlation at 720 nm, indicating that estimators at 495 nm and 720 nm should be considered for elimination. Feature selection can be performed automatically using regularization regression, such as Ridge regression, as shown in the correlation heatmap in Figure 4. Ridge regression can select the most important features and reduce the coefficient of the least important feature if two features are linearly correlated. The L2 regularization performed by Ridge regression adds a penalty equal to the square of the coefficient to the minimization target, which affects the cost function based on the chosen alpha. Table 1 summarizes the regression coefficients of Cu(II), Fe(III), and Ni(II) at each maximum wavelength as a function of alpha 0.01 and 0.1. The Cu(II) Ridge regression model yielded a coefficient of -0.718 at 395 nm for alpha = 0.01. Fe(III) did not show a reliable correlation with any absorbance wavelength according to Ridge regression, and the weighting decreased as alpha increased. A lower alpha resulted in a regression model more like ordinary linear regression.

TABLE I. The ridge regression weight at each wavelength as a function of alpha

Alpha		0.01			0.1	
Wavelength (nm)	Cu Coef.	Fe Coef.	Ni Coef.	Cu Coef.	Fe Coef.	Ni Coef.
805	3.2820	-0.0131	-2.2297	2.6155	-0.0105	-1.5477
295	0.4295	-0.0017	1.3165	0.5889	-0.0024	2.6741
495	0.2195	-0.0009	-1.7957	-0.1967	0.0008	0.2919
720	1.2298	-0.0049	2.8400	1.3091	-0.0052	0.2815
395	-1.9173	0.0077	6.6963	-1.7446	0.0070	4.7705

The Ridge regression slope values at 495 nm and 720 nm provided a way to eliminate these estimators. To ensure the reliability of the regression models, the intercept and slope of both Linear and Ridge regressions of each Cu(II), Fe(III), and Ni(II) were sampled 1000 times using the No-U-Turn Sampler (NUTS) with a posterior distribution assumption. The slope and intercept were assumed to be normally distributed with a standard deviation of the half-Cauchy distribution. The PyMC3 library in Python was used for inference [16]. The comparison of the slope distributions for Cu(II), Fe(III), and Ni(II) between the linear and ridge models is presented in Figure 5. The determination of Cu(II) was more precise, with a smaller standard deviation. The slope at 805 nm gave a positive value, while the slope at 395 nm gave a negative value. The absorbance at 295 nm did not significantly contribute to the regression models, as its value was close to zero. The slope of the Ridge model was more centered around 0.0, as shown in Figure 5(a). The slope distribution for Fe(III) and Ni(II) showed the same pattern in both linear and ridge models, as depicted in Figures 5(b) and 5(c). The slope of both Fe(III) and Ni(II) at 805 nm gave a negative value, and the slopes at 295 nm, 395 nm, and 495 nm did not significantly contribute, as their values were close to zero. Table 2 displays the prediction recoveries of the linear regression and Ridge (alpha=0.1) models generated using absorbance estimators at wavelengths 295 nm, 395 nm, and 805 nm. The dataset was split into a training set (80%) and a test set (20%) to evaluate the accuracy of the models.

TABLE II. Linear and ridge regression recoveries using estimated absorbances at 295, 395, and 805 nm

Compounds	Linear	Ridge
Cu	100.64	101.90
Fe	98.13	97.77
Ni	98.13	97.77

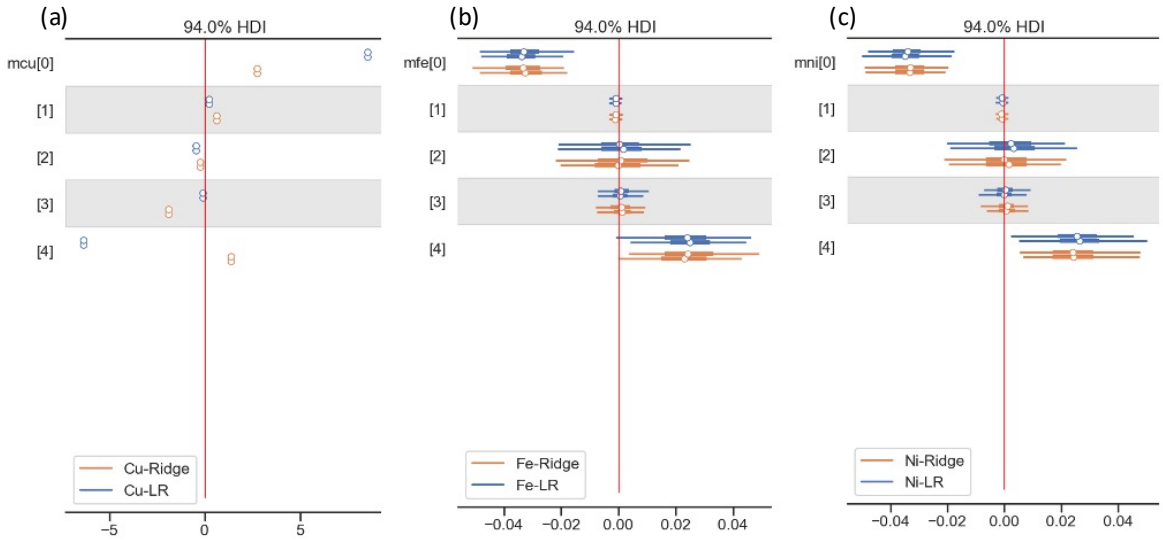

Figure 5. Forest plot of the Linear and Ridge regression model slope distributions of Cu(II) (a), Fe(III) (b), and Ni(II) (c) with 5 estimators.

Figure 6 presents a boxplot of the recovery values for Cu(II), Fe(III), and Ni(II) using the linear and Ridge(alpha=0.1) regression models with absorbance at wavelengths 295, 395, and 805 nm as estimators. The boxplot shows that the determination of Fe(III) and Ni(II) using the linear model has a larger interquartile range (IQR) compared to the Ridge model, which skews the curve towards the maximum value. On the other hand, the determination of Cu(II) shows better precision and accuracy with a smaller IQR for both models, as seen in the boxplot. However, there was no significant difference in the recoveries obtained using the Ridge and linear regression models.

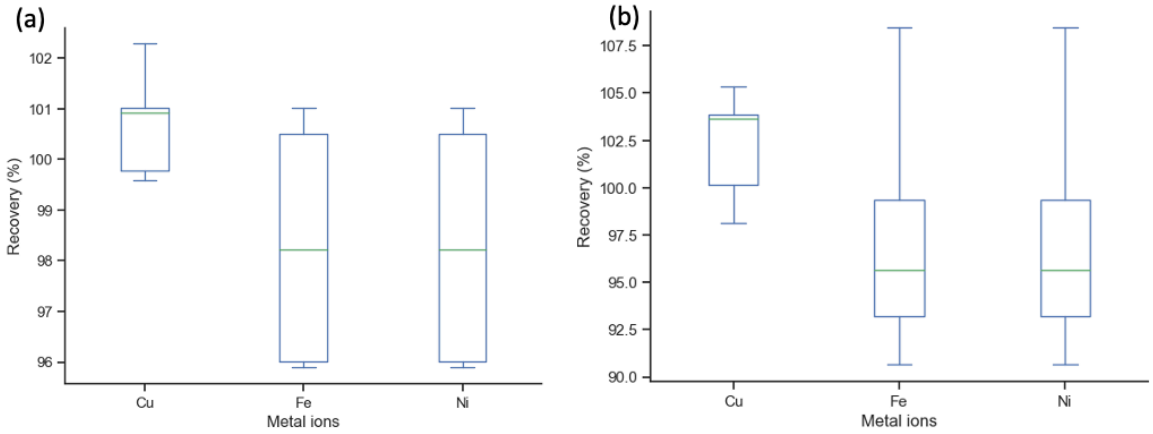

Figure 6. The (a) Linear and (b) Ridge regression recoveries of Cu(II), Fe(III), and Ni(II)

To validate the accuracy of the model, a test solution was prepared outside of the training dataset. Three replications of the test solution were measured in the same wavelength range, and their spectra are shown in Figure 7.

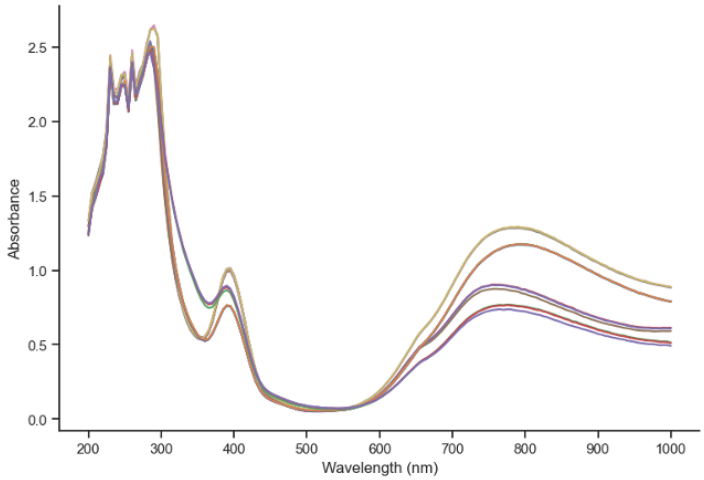

Figure 7. Spectra of test solutions containing Cu(II), Fe(III) and Ni(II) with concentration variations of [5, 0.008 and 8 mg/L] and [3, 0.008 and 8 mg/L]

Figure 8 displays the predictions of the linear and ridge regression models for Cu(II), Fe(III), and Ni(II) using the test solution.

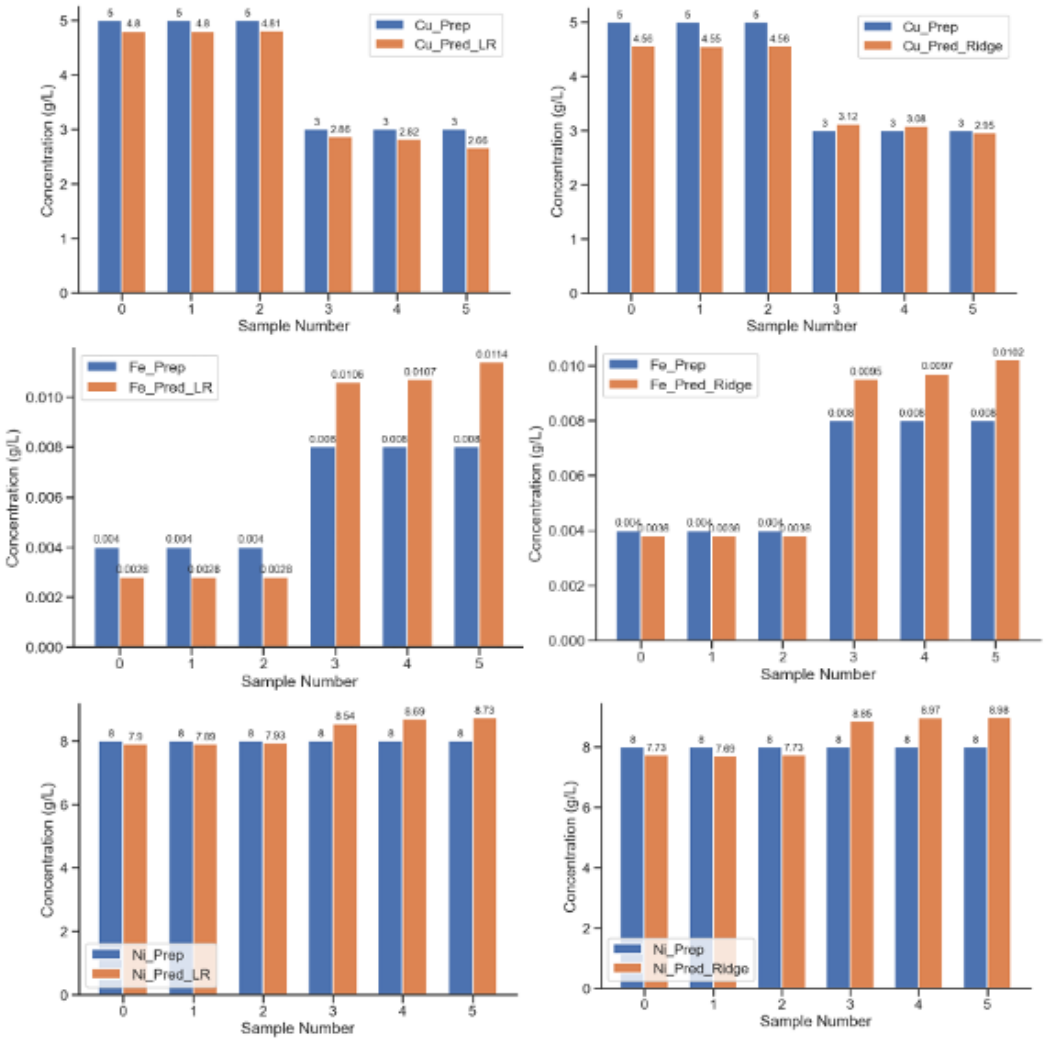

Figure 8. Test solution prediction of Cu(II), Fe(III) and Ni(II)

The linear and ridge regression models' mean recoveries for Cu(II), Fe(III), and Ni(II) in the test solutions were calculated and found to be 94.36%, 102.87%, and 103.51% for the linear model, and 96.37%, 108.56%, and 104.07% for the ridge model, respectively. In addition, a further analysis was conducted using only three estimators at wavelengths 295, 395, and 805 nm to investigate the impact of one ion absorption on another. The estimator at 495 and 720 nm was excluded, and the resulting slope value was found to be close to 0, indicating that this variable did not significantly affect the regression equations' predictions. Figure 9 shows the slope's value, supporting this finding. Box plots of linear and Ridge regression models for Cu(II), Fe(III), and Ni(II) using typical absorption of each ion, without eliminating the influence of other ion absorption, are shown in Figure 10 (a-f).

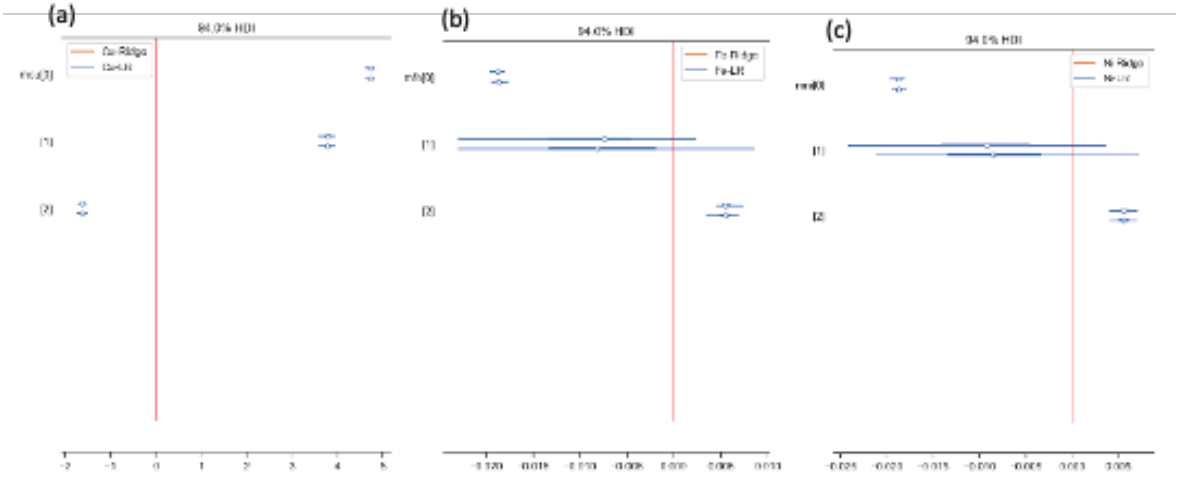

Figure 9. Forest plot of linear and ridge regression model slope distributions of Cu(II) (a), Fe(III) (b), and Ni(II) (c) with 3 estimators

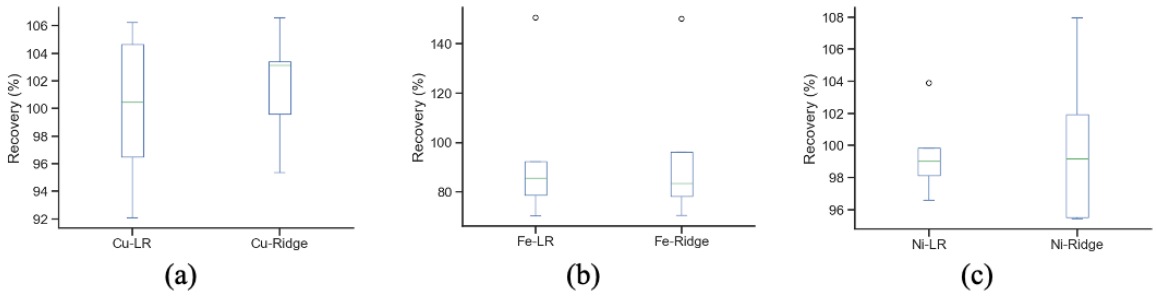

Figure 10. Boxplot of linear and ridge regression model of Cu(II) (a), Fe(III) (b), and Ni(II) (c) for 20% test solution

The linear and ridge regression models based only on the absorbance at 805 nm were used to predict the mean recoveries for Cu(II), Fe(III), and Ni(II) in test data and a test solution outside of the training data. The mean recoveries for Cu(II) using linear and ridge regression in the 20% test data were 99.97% and 101.6%, respectively. For Fe(III), the mean recoveries using linear and ridge regression in the 20% test data were 95.42% and 95.65%, respectively. The mean recoveries for Ni(II) using linear and ridge regression in the 20% test data were 99.43% and 99.99%, respectively. For the test solution outside of the training data, the mean recoveries for Cu(II) using linear and ridge regression based only on absorbance at 805 nm were 92.27% and 95.03%, respectively. The mean recoveries for Fe(III) using linear and ridge regression based only on absorbance at 805 nm were 125.3% and 124.11%, respectively. For Ni(II), the mean recoveries using linear and ridge regression based only on absorbance at 805 nm were 104.15% and 105.52%, respectively. The boxplot for the out-of-sample test solution is shown in Figure 11.

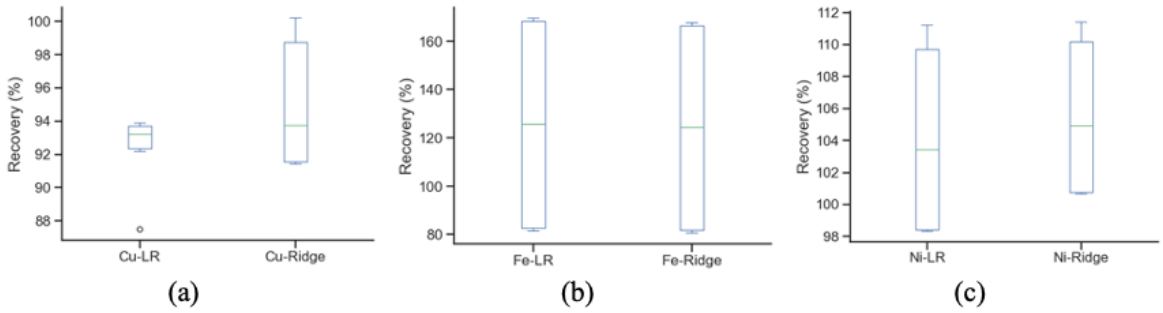

Figure 11. Boxplot of the linear and ridge regression model of Cu(II) (a), Fe(III) (b), and Ni(II) (c) for out-of-sample test solutions

4. CONCLUSION

In conclusion, the UV-Vis spectrophotometric method used in this study is an efficient and accurate way to determine the metal ion content of Cu(II) and Ni(II) in multicomponent samples without prior complexation or separation. The regression models obtained through single and multivariate regression analyses provide comprehensive predictions of metal ion content. The mean recoveries for Cu(II), Fe(III), and Ni(II) indicate that the linear and ridge regression models based only on absorbance at 805 nm have high accuracy for both test data and test solutions outside of the training data. Overall, the results demonstrate that the multivariate UV-Vis spectrophotometric method is suitable for the simultaneous determination of Cu(II) and Ni(II) in multicomponent samples and can be applied successfully in various analytical fields.

Acknowledgment

The authors gratefully acknowledge financial support from the Institut Teknologi Sepuluh Nopember for this work, under the project scheme of the Publication Writing and IPR Incentive Program (PPHKI) 2023.

References

[1] J. Chen, C. Yang, H. Zhu, Y. Li and J. Gong J., "Simultaneous determination of trace amounts of copper and cobalt in high concentration zinc solution using UV–vis spectrometry and Adaboost," *Optik*, vol. 181, pp. 703–713, 2019.

[2] F. Zhou, C. Li, H. Zhu, and Y. Li, "A novel method for simultaneous determination of zinc, nickel, cobalt, and copper-based on UV–vis spectrometry", *Optik,* vol. 182, pp. 58-64, 2019.

[3] S. El Fadeli, R. Bouhouch, A. El-Abbassi, M. Lahrouni, F. Aziz, H. Benmazhar, M. B. Zimmermann, and A. Sedki, "Assessment of heavy metals contamination in soils around a mining site in Marrakech region, Morocco", *Moroccan Journal of Chemistry*, vol. 3(4), pp. 741-747, 2015.

[4] D. Xu, W. Fan, H. Lv, Y. Liang, Y. Shan, G. Li, Z. Yang and L. Yu, "Simultaneous determination of traces amounts of cadmium, zinc, and cobalt-based on UV–Vis spectrometry combined with wavelength selection and partial least squares regression", *Spectrochimica Acta Part A: Molecular and Biomolecular Spectroscopy,* vol. 123, pp. 430–435, 2014.

[5] L.O. dos Santos, G.C. Brandao, A. M. P. dos Santos, S. L. C. Ferreira and V. A. Lemos, "Direct and Simultaneous Determination of Copper and Iron in Flours by Solid Sample Analysis and High-Resolution Continuum Source Graphite Furnace Atomic Absorption Spectrometry", *Food Analytical Methods,* vol. 10(2), pp. 469–476, 2017.

[6] D. L. F. da Silva, M.A. P. da Costa, L. O. B. Silva and dos W. N. L. Santos, "Simultaneous determination of mercury and selenium in fish by CVG AFS", *Food Chemistry*, vol. 273, pp, 24–30, 2019.

[7] F. Cheng, C. Yang, C. Zhou, L. Lan, H. Zhu and Y. Li, "Simultaneous Determination of Metal Ions in Zinc Sulfate Solution Using UV–Vis Spectrometry and SPSE-XGBoost Method", *Sensors*, vol. 20(17), pp. 4936, 2020.

[8] F. Zhou, C. Li, H. Zhu and Y. Li, "Determination of trace ions of cobalt and copper by UV–vis spectrometry in purification process of zinc hydrometallurgy", *Optik*, vol. 184, 227-233, 2019.

[9] S. Yasar S. and R. Tosun, "Predicting chemical, enzymatic and nutritional properties of fermented barley (Hordeum vulgare L.) by second derivate spectra analysis from attenuated total reflectance-Fourier transform infrared data and its nutritional value in Japanese quails", *Archives of Animal Nutrition*, vol. 72(5), pp. 407–423, 2018.

[10] S. Asadollahi, M.R. Sohrabi and S. Mofavvaz, "Rapid Simultaneous Spectrophotometric Determination of Food Dyes in Soft Drink Using Continuous Wavelet Transform and Multivariate Calibration Methods", *Iranian Journal of Chemistry and Chemical Engineering,* vol. 41(5), pp. 1682-1693, 2022.

[11] F. M. Fernández, M. B. Tudino, and O. E. Troccoli, "Multicomponent kinetic determination of Cu, Zn, Co, Ni, and Fe at trace levels by first and second order multivariate calibration", *Analytica Chimica Acta*, vol. 433(1), pp. 119-133, 2001.

[12] S. Agarwal S. G. Aggarwal, and P. Singh, "Quantification of ziram and zineb residues in fog-water samples", *Talanta,* vol. 65(1), pp. 104-110, 2005.

[13] A.C. B. Dias, J. M. T. Carneiro, V. Grassi, and E. A. G. Zagatto, "High-sensitivity methods for sequential injection determination of the main constituents of alloys", *Analytica Chimica Acta,* vol. 514(2), pp. 253-257, 2004.

[14] X. Yan and X. Su, "*Linear Regression Analysis: Theory and Computing"*, World Scientific; New Jersey, USA, 2009.

[15] I.S. Dar, S. Chand, M. Shabbir, and G. M. B. Kibria, "Condition-index based new ridge regression estimator for linear regression model with multicollinearity", *Kuwait Journal of Science*, vol. 50(2), pp. 91-96, 2023.

[16] J. Salvatier, T. V. Wiecki and C. Fonnesbeck, "Probabilistic programming in Python using PyMC3", *PeerJ Computer Science*, vol. 2, pp. 55, 2016.